Organic Geochemistry 176 (2023) 104544

Contents lists available at ScienceDirect

Organic Geochemistry

journal homepage: www.elsevier.com/locate/orggeochem

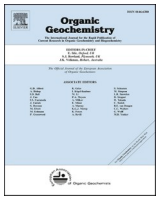

Identification, distribution and geochemical significance of phenyldibenzofurans in coals

Jiayang Li [a,b], Zhihuan Zhang [a,b,*], Zhili Zhu [c]

[a] State Key Laboratory of Petroleum Resources and Prospecting, China University of Petroleum (Beijing), Beijing 102249, China
[b] College of Geosciences, China University of Petroleum (Beijing), Beijing 102249, China
[c] Wuxi Research Institute of Petroleum Geology, RIPEP, SINOPEC, Wuxi, Jiangsu 214216, China

ARTICLE INFO

Associate Editor–Kliti Grice

Keywords:
Phenyldibenzofuran
Thermodynamic stability
Maturity indicator
Coal

ABSTRACT

Four phenyldibenzofuran (PhDBF) isomers were unambiguously identified for the first time in coals through co-injection of commercially available standards. PhDBF isomers were detected in all coals from the East China Sea Shelf and the Ordos basins. The stability order of PhDBFs was confirmed to be 4-PhDBF > 2-PhDBF > 3-PhDBF > 1-PhDBF. The degree of molecular structural deformation of PhDBFs was also determined. The influence of thermal maturity on the distributions of PhDBFs in sedimentary organic matter containing Type II–III kerogen was systematically investigated, and the concentration of 4-PhDBF relative to 2-PhDBF and 3-PhDBF was found to be influenced by thermal maturation. The previously proposed maturity indices based on PhDBF ratios (PhFR-1 and PhFR-2) were found to be useful in coal facies with high thermal maturity (≥ 1.0 %Ro) on the basis of density functional theory (DFT) calculations and geochemical data. Two calibrations of PhFR-1 and PhFR-2 against the measured vitrinite reflectance (%Ro) were established, which are as follows: %Rc = 3.0 × PhFR-1/100 + 1.0 (≥ 1.0 %Ro) (R^2 = 0.95) and %Rc = 7.0 × PhFR-2/100 + 1.0 (≥ 1.0 %Ro) (R^2 = 0.96). PhFR-1 and PhFR-2 have good correlations with the other widely used thermal maturity indicators. The oxic sedimentary environment is likely more beneficial to the generation of phenyldibenzofurans and methyldibenzofurans. PhDBFs in coals may be formed during diagenesis or early catagenesis and intermediates in the producing of more condensed aromatic compounds from high thermal maturity. The results of this study provide a deeper insight into the occurrence, distribution and significance of PhDBFs in sedimentary deposits.

1. Introduction

Methyldibenzofurans (MDBFs) and their corresponding phenyl substituted counterparts (phenyldibenzofurans) are important oxygen-containing heterocycles found in crude oils and ancient sedimentary rocks (e.g., Radke et al., 2000; Marynowski et al., 2002; Li and Ellis, 2015; Yang et al., 2017; Li et al., 2018). However, compared with MDBFs, the distributions of PhDBFs and their application in petroleum geochemistry have received less attention.

Three unidentified phenyldibenzofuran (PhDBF) isomers and 3-PhDBF were first detected in furnace gases and coal tar pitches (Meyer zu Reckendorf, 1997). Later, four PhDBF isomers were identified by injection of commercially available standards (Meyer zu Reckendorf, 2000; Marynowski et al., 2002). Moreover, PhDBFs were reported in charcoal-bearing sediments, shales, carbonates and crude oils (Marynowski and Simoneit, 2009; Grafka et al., 2015; Yang et al., 2017; Ogbesejana and Bello, 2020). The occurrence and identification of PhDBFs in coals has not been extensively appraised.

The origin and formation mechanism of PhDBFs are controversial. Fields and Meyerson (1967) suggested that the formation of PhDBFs involved a phenyl radical mechanism from pyrolysis of nitrobenzene. Marynowski et al. (2002) also suggested phenyl free radical substitution of DBF can lead to the formation of 1-PhDBF (Southwick et al., 1961). Meyer zu Reckendorf (2000) proposed PhDBFs are intermediates in the transformation of dibenzofuran (DBF) into benzobisbenzofuran and triphenyleno[1,12-*bcd*]furan via a pyrolysis process. Marynowski et al. (2001) reported PhDBFs may be derived from carbohydrates. Marynowski et al. (2002) proposed that PhDBFs are formed by diagenetic/catagenetic oxidation of organic matter in sedimentary rocks. Marynowski and Simoneit (2009) proposed that PhDBFs in charcoal-bearing sediments are formed during combustion processes.

MDBFs are useful markers in petroleum geochemistry. The

* Corresponding author at: State Key Laboratory of Petroleum Resources and Prospecting, China University of Petroleum, Beijing 102249, China.
E-mail address: zhangzh3996@vip.163.com (Z. Zhang).

https://doi.org/10.1016/j.orggeochem.2022.104544
Received 16 August 2022; Received in revised form 20 December 2022; Accepted 26 December 2022
Available online 29 December 2022

distribution characteristics of MDBFs are mainly controlled by the organic matter type of source rock and paleoenvironment (Fan et al., 1991; Radke et al., 2000; Li et al., 2013; Li and Ellis, 2015). MDBFs tend to more abundant in terrestrial source rocks and coals (Fan et al., 1991; Li et al., 2013). The abundance of alkyldibenzofurans relative to alkyldibenzothiophenes was widely used to establish paleoenvironments of deposition (Sephton et al., 1999; Kruge et al., 2000; Radke et al., 2000). Recently, Li et al. (2018) proposed 1-MDBF/4-MDBF as an indicator of oil migration pathways. Whether the MDBF ratio (4-MDBF/1-MDBF) can be used as a thermal maturity indicator is still controversial. For example, Radke et al. (2000) proposed a maturity indicator, i.e., 1-MDBF/4-MDBF, which significantly increases with increasing vitrinite reflectance (> 1.0 %Ro). In contrast, Li et al. (2011, 2018) observed that there was no obvious relationship trend of 1-MDBF/4-MDBF with increasing thermal maturity. The origin and formation mechanism of MDBFs in sedimentary organic matter still remain controversial. Previous studies reported that MDBFs are likely to originate from lignin-containing plants, phenols, and polysaccharides (Born and Mulder, 1989; Sephton et al., 1999; Fenton et al., 2007). Radke et al. (2000) proposed that MDBFs in sedimentary organic matter are likely sourced from lichens. In addition, Asif et al. (2010) demonstrated that MDBFs in sediments may originate from biphenyl based on geochemical data and controlled laboratory experiments with standard components.

The geochemical applications of PhDBFs have been preliminarily investigated. For example, Marynowski et al. (2002) showed that the maturation trend observed for PhDBFs distributions is equivocal. Lower maturity (< 0.8 %Ro) samples contain either 2-PhDBF or 4-PhDBF as the dominant isomer and the samples (only two) of higher maturity (> 1.0 % Ro) show an abundant 4-PhDBF isomer. Marynowski et al. (2002) also inferred that fluctuations in distributions of PhDBFs are similar to MDBF distribution, for which maturity dependent trends are observed > 1.0 % Ro (Radke et al., 2000). Grafka et al. (2015) found the PhDBFs from relative high maturity samples with calculated values of %Ro > 1.3 are dominated by 4-PhDBF. Other PhDBF isomers are only observed in trace abundances or are absent, confirming that the relationship between the distributions of PhDBFs and thermal maturity is unclear. However, Yang et al. (2017) observed that the relative abundances of 2-PhDBF and 3-PhDBF to 4-PhDBF generally decrease with increase in thermal maturity (0.32–1.43 %Ro). They assigned PhDBF ratios (PhFR-1 = 4-PhDBF/2-PhDBF and PhFR-2 = 4-PhDBF/(2-PhDBF + 3-PhDBF)) as thermal maturity indicators. Ogbesejana and Bello (2020) confirmed that PhFR-1 and PhFR-2 can be used as thermal maturity indicators, which gradually increase with rising burial depth and show very good correlations with calculated vitrinite reflectance. These recent studies contradict earlier reports (Marynowski et al., 2002; Grafka et al., 2015) probably because maturation ranges of the investigated samples are not wide enough to show the behavior of PhDBFs at comparatively low maturity to relative high maturity. Based on the distribution characteristics of PhDBFs in the samples with different thermal histories reported by previous studies, the abundances of 2-PhDBF and 3-PhDBF relative to 4-PhDBF decrease with increasing thermal maturity, suggesting that PhDBF ratios are potential thermal maturity indicators. However, PhFR-1 and PhFR-2 have not been established as quantitative formulae for practical application in thermal maturity evaluation.

In this paper, PhDBFs were firmly identified in coals for the first time through injection of authentic standards. We conducted density functional theory (DFT) calculations to obtain the thermodynamic properties of PhDBFs. Then, we describe the distribution characteristics of PhDBFs in coals from the Xihu Depression (East China Sea Basin) and the Ordos Basin. The application of PhDBFs for thermal maturity evaluation is discussed. The formation mechanism and origin of PhDBFs in coals were also preliminarily investigated.

2. Geologic setting and samples

The 240 × 10^3 km^2 East China Sea Basin (ECSB) is an important offshore petroliferous basin in China (Fig. 1a) (Li and Li, 2003; Li et al., 2004). The Xihu Depression, covering an area of 4.6 × 10^3 km^2, located northeastern ECSB (Fig. 1c), is rich in oil resources and believed to be highly prospective for hydrocarbon exploration (Ye et al., 2007). Previous studies reached the consensus that the coal-bearing Eocene Pinghu Formation (E_2p) is the major source rock unit, and both coals and carbonaceous mudstones contribute to the hydrocarbon accumulations (Li et al., 2004; Zhu et al., 2012; Cheng et al., 2020). The Pinghu Formation was extensively distributed and developed in a lacustrine–swamp depositional environment within a semi-enclosed bay (Chen, 1998; Zhu et al., 2012).

The E_2p unit is mainly composed of siltstone, mudstone, carbonaceous mudstone and coal (Tao and Zou, 2005; Cheng et al., 2019). Fourteen coals from the Xihu Depression were sampled in the Pinghu Formation. The coals have high total organic carbon (TOC) content, which range from 37.1% to 74.5%. The hydrocarbon generation potential ($S_1 + S_2$) and the hydrogen index (HI) of the coals are in the ranges of 50–235 mg/g and 120–370 mg HC/g TOC, respectively.

The EOM (extractable organic matter) of coal samples range from 11.5 mg/g C_{org} to 160 mg/g C_{org}. The Tmax values and vitrinite reflectances of the coals are in the ranges of 421–461 °C and 0.60–1.00 % Ro, respectively, suggesting that they are of relatively low maturity to high maturity (Table 1). Based on Tmax versus HI plot, the coals mainly consist of Type II–III kerogen. The pristane/phytane (Pr/Ph) values of the coal samples are high with values ranging from 4.95 to 8.82 (Table 2).

The Ordos Basin is a large Mesozoic depression and located in north-central China (Fig. 1a) (Li, 1995). Previous studies suggested that the source rocks of the Upper Paleozoic gas reservoir are Carboniferous–Permian (C—P) coals and mudstones (Dai et al., 2005; Hu et al., 2010). These Carboniferous–Permian source rocks cover an area of 180 × 10^3 km^2 and are widely distributed in the basin (Dai et al., 2005; Shuai et al., 2013; Zou et al., 2013). The Carboniferous–Permian stratum were mainly deposited in marine–terrestrial transitional environment, and mainly contain sandstones, shales and coals (Ding et al., 2013; Zhao et al., 2014). The Carboniferous–Permian stratum was altered by hydrothermal fluid from Early Cretaceous volcanic activity (Yang et al., 2005). In this basin, we collected 16 coal samples from Carboniferous–Permian formations (Fig. 1b). These samples have TOC, HI, EOM and Tmax values of 68.6–91.5%, 48.8–277 mg HC/g TOC, 2.69–137 mg/g C_{org} and 435–505 °C, respectively. Judging from HI and Tmax values, these coal samples are mainly comprised of Type II–III kerogen. The coal samples are characterized by higher maturity (0.62–1.88 %Ro; Table 1) and low Pr/Ph values of 0.49–2.00 (Table 2).

3. Methods and reference compounds

3.1. Experimental methods

The coal samples were crushed to < 80 mesh (0.2 mm) in diameter. Rock-Eval pyrolysis were carried out on the OGE Pyrolysis Apparatus yielding results similar to the traditional Rock-Eval pyrolysis analyzer (Zhu et al., 2019, 2022). Before analysis, contaminants and carbonates were removed from the coals with deionized water and HCl, respectively. Then, the LECO CS-230 carbon/sulfur apparatus was used to obtain the TOC content. The vitrinite reflectances of coals were measured on a Leica Model MPV-SP microscopic photometer on the basis of the method of Kilby (1988).

The powdered coals were extracted for 48 h in a Soxhlet apparatus using 400 mL of dichloromethane/methanol (93:7, v/v). Asphaltenes were removed from the extracts by precipitation using *n*-heptane and then fractionated into saturated, aromatic, and resin fractions by liquid chromatography using alumina/silica gel columns. The elution solvents used were petroleum ether, dichloromethane:petroleum ether (2:1, v/v), and dichloromethane:methanol (93:7, v/v). The analyses of authentic standards and aromatic fractions were carried on an Agilent

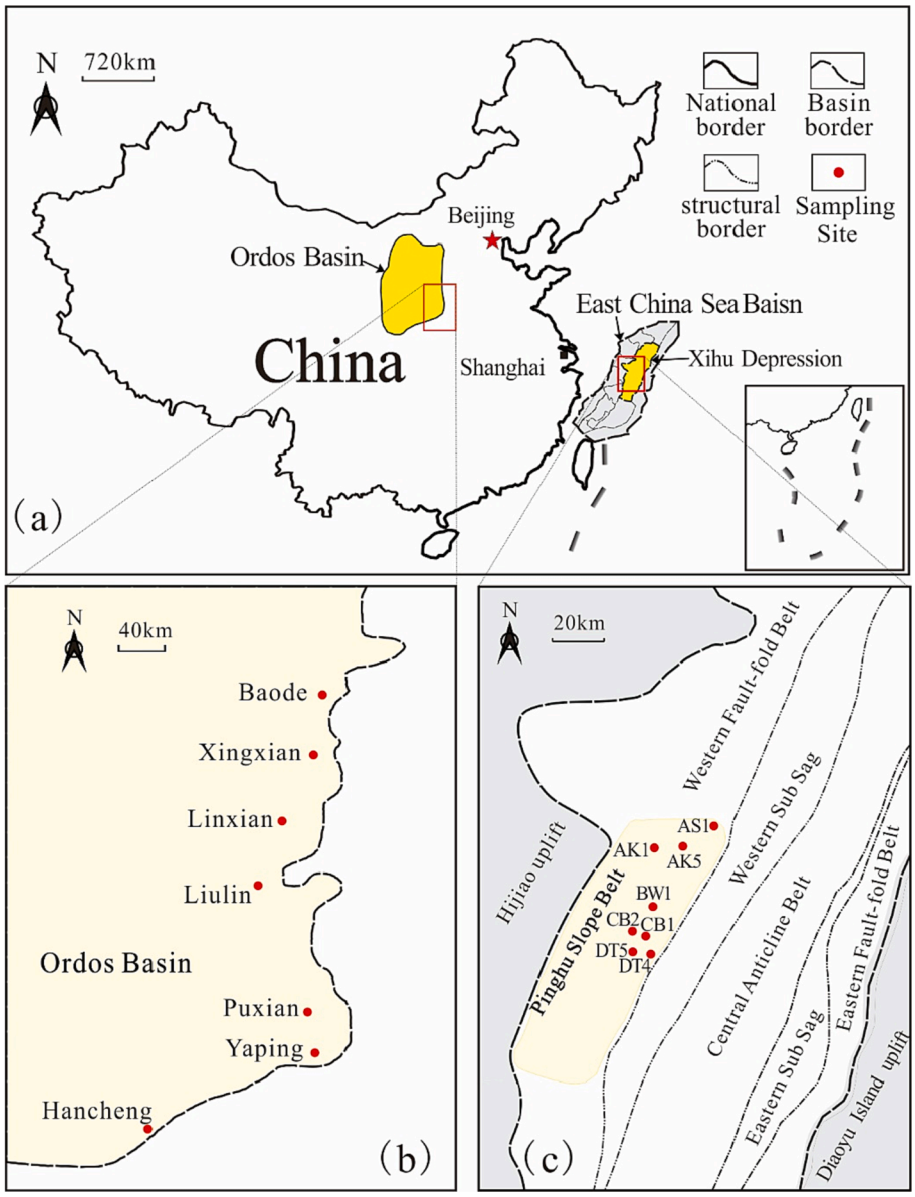

Fig. 1. Sampling sites and well locations for samples analyzed in this study.

6890 gas chromatograph coupled to a 5975i MS equipped with a HP-5MS column (60 m × 0.25 mm i.d., 0.25 μm film thickness). The gas chromatography–mass spectrometry (GC–MS) operating conditions were as follows: initial temperature was kept at 80 °C for 1 min, then raised to 310 °C at 3 °C/min, and finally held isothermal for 16 min. Helium was the carrier gas and the temperature of injector was set at 300 °C. The mass spectrometer was used in electron impact (EI) mode with ionization energy of 70 eV and a scan range of 50–600 Da.

3.2. Authentic standards and quantification of aromatic compounds

We purchased four commercially available PhDBF isomers (1-PhDBF, 2-PhDBF, 3-PhDBF, 4-PhDBF) from Chiron AS, Norway. We also added phenanthrene and chrysene to the mixtures of PhDBF standards as markers to calculate the retention indices of PhDBFs in the GC–MS analysis. Furthermore, we added a known amount of phenanthrene-d_{10} to samples as an internal standard. The m/z 188 mass chromatogram was used to detect and qualify the phenanthrene-d_{10}. MDBFs and PhDBFs were quantitated by integration of mass chromatograms of m/z 182 and m/z 244, respectively. By comparison with amount of phenanthrene-d_{10}, the contents of MDBFs and PhDBFs are determined.

3.3. Calculation methods

The density functional theory (DFT) calculation is a good method for investigating geochemical phenomena in petroleum geochemistry (Yang et al., 2019; Zhu et al., 2019, 2022; Liu et al., 2020). In this paper, we applied DFT calculations to determine thermodynamic properties, i.e., Gibbs free energy (ΔG), enthalpy (ΔH), electron energy (ΔE), and internal energy (ΔU), at the B3LYP/6–311++G (d,p.) level of gas phase at 25 ℃. In order to show the difference of the thermal stability of PhDBF isomers, all thermodynamic energies are defined as relative values compared to the isomer with the lowest energy, which means that ΔG, ΔH, ΔE and ΔU are expressed relative to the lowest energy isomer. The relative energy (e.g., ΔG) of the lowest energy isomer is defined as 0.00 kcal/mol, and the relative energy of other isomers can be determined by subtracting the absolute energy of the lowest energy isomer from its absolute energy. The relative energy (e.g., ΔG) of the isomer is greater, suggesting it is more unstable. The geometric optimizations were also obtained by using the calculation method B3LYP/6–311++G (d,p.) (Zhu

Table 1
Geochemical characteristics of coals in this study.

Basin	Sampling Site	Sample Name	Formation	Type	TOC (%)	Tmax (°C)	% Ro	HI (mg HC/g TOC)	$S_1 + S_2$ (mg/g)	EOM (mg/g C_{org})
East China Sea Basin	Xihu Depression	CB2-1	E_2p	Core	56.5	421	0.60	370	217	108
		AK1-1	E_2p	Core	39.0	428	0.64	288	118	104
		BW1-1	E_2p	Cutting	62.6	427	0.63	232	150	50.1
		CB1-1	E_2p	Core	38.1	433	0.67	366	143	95.0
		DT4-1	E_2p	Core	74.5	437	0.74	212	168	160
		BW1-2	E_2p	Cutting	39.2	430	0.69	244	101	92.8
		CB1-2	E_2p	Core	61.0	433	0.70	356	236	133
		AS1-1	E_2p	Cutting	37.1	461	1.00	120	50.1	52.8
		CB2-2	E_2p	Cutting	57.3	429	0.62	194	130	121
		AK5-1	E_2p	Cutting	65.0	460	0.96	193	140	11.5
		DT5-1	E_2p	Cutting	53.9	436	0.72	266	157	64.5
		AK1-2	E_2p	Cutting	45.3	437	0.74	195	93.7	35.0
		CB1-3	E_2p	Cutting	44.6	438	0.76	203	99.8	61.6
		AK1-3	E_1p	Cutting	58.6	457	0.88	192	124	16.9
Ordos Basin	Baode	BDS24	C—P	Outcrop	68.6	444	0.62	246	171	74.3
		BDS14	C—P	Outcrop	73.9	444	0.71	235	176	71.8
	Linxian	LXS11	C—P	Outcrop	77.9	444	0.77	239	192	78.2
		LXS15	C—P	Outcrop	91.5	463	0.96	176	166	11.1
		LXS8	C—P	Outcrop	71.2	455	1.03	194	139	17.4
	Xingxian	XXS10	C—P	Outcrop	74.3	440	0.73	278	209	69.1
		XXS2	C—P	Outcrop	85.4	492	1.35	120	106	8.36
	Liulin	LLS25	C—P	Outcrop	84.3	493	1.40	97.4	82.7	7.84
		LLS26	C—P	Outcrop	84.3	493	1.24	116	105	11.0
		LLS5	C—P	Outcrop	75.1	489	1.27	96.9	75.6	15.1
	Hancheng	HCS1	C—P	Outcrop	80.7	498	1.66	62.9	51.7	2.69
		HCS13	C—P	Outcrop	85.4	505	1.57	53.0	46.6	4.94
		HCS4	C—P	Outcrop	83.8	501	1.88	48.8	41.9	4.78
	Puxian	PXS22	C—P	Outcrop	83.1	435	0.62	276	243	138
		PXS6	C—P	Outcrop	84.3	444	0.63	230	204	88.7
	Yaping	YPS9	C—P	Outcrop	82.4	484	1.36	107	90.0	12.7

TOC: total organic carbon; Tmax: temperature at maximum generation; %Ro: vitrinite reflectance value; HI: hydrogen index = $S_2 \times 100$/TOC; EOM: extractable organic matter.

et al., 2019, 2022). We used Gaussian 09 program for DFT calculations (Yang et al., 2019; Zhu et al., 2019, 2022).

4. Results and discussion

4.1. Identification and thermodynamic stability of phenyldibenzofurans

All four PhDBF isomers were unequivocally identified in coals using the injection of commercially available standards. The elution order of PhDBFs is as follows: 1-PhDBF, 4-PhDBF, 2-PhDBF, 3-PhDBF (Fig. 2), which is in agreement with previous studies (Meyer zu Reckendorf, 2000; Marynowski et al., 2002; Yang et al., 2017). We also used the retention index system (Kováts, 1958; Van den Dool and Kratz, 1963) and accurately calculated the retention indices of PhDBF isomers according to the equation proposed by Lee et al. (1979). The calculated $I_{HP\text{-}5MS}$ retention indices of PhDBF isomers are identical to those reported by Yang et al. (2017).

The calculated thermodynamic properties of PhDBFs show that their thermodynamic stabilities increase following the sequence: 1-PhDBF < 3-PhDBF < 2-PhDBF < 4-PhDBF (Table 3), which is in agreement with data reported by Yang et al. (2017) and Meyer zu Reckendorf (2000). Previous studies suggested that steric hindrance may cause the difference in thermodynamic stability for phenyl polycyclic compounds (Yang et al., 2019; Zhu et al., 2019, 2022). The thermodynamic instability, caused by the phenyl ring at C-4 to C-1, results from steric hindrance (Fig. 3). With regard to 1-PhDBF, these angles between the phenyl ring and the dibenzofuran (DBF) group are obviously deformed from the ideal 120° (Fig. 3a). This causes the increase of total energy and makes it unstable. For 2-PhDBF and 3-PhDBF, these corresponding angles are less deformed, resulting in the decrease of total energy and instability. The angles of 4-PhDBF are severely deformed and the deformation degree is higher than that of the other three PhDBF isomers (Fig. 3d). Significantly, the lone pair of electrons of the oxygen atom are able to form a hydrogen bond with the hydrogen atom of the phenyl ring at C-4 in the dibenzofuran ring, which makes it the most stable isomer. The bond length of H—O is 2.560 Å, which is within the range of a hydrogen bond. Li et al. (2018) suggested that hydrogen bond (2.970 Å) between the oxygen atom in 4-methyldibenzofuran and the hydrogen atom of methyl can readily form.

4.2. Effects of thermal maturity on the distributions of phenyldibenzofurans

Fig. 4 illustrates the distribution characteristics of PhDBFs in the coal samples with various thermal maturities. Most samples contain a very low abundance of 1-PhDBF, which may be attributed to its lower thermodynamic stability. The coals with thermal maturity < 1.0 %Ro contain 2-PhDBF or 4-PhDBF as the dominant isomer, while 3-PhDBF is present in relatively low abundance (Fig. 4a–c). Similarly, in carbonates and shales with thermal maturity < 0.6 %Ro, 2-PhDBF prevails over 3-PhDBF and 4-PhDBF. When the thermal maturity exceeds 0.6 %Ro, the abundance of 4-PhDBF is relatively high and significantly higher than that of 2-PhDBF and 3-PhDBF (Marynowski et al., 2002; Yang et al., 2017). The coals with thermal maturity > 1.0 %Ro contain 4-PhDBF as the dominant isomer, while 2-PhDBF and 3-PhDBF are present in relatively low abundances (Fig. 4d,e). Coincidentally, for the more mature shales and carbonates (> 1.0 %Ro), 4-PhDBF dominates in the samples, while 2-PhDBF and 3-PhDBF are in very low concentrations or are nearly absent (Marynowski et al., 2002; Grafka et al., 2015; Yang et al., 2017). The above phenomena suggests that the distribution characteristics of PhDBFs in the coals of this study are consistent with previous research. Therefore, the concentration of 4-PhDBF relative to 2-PhDBF and 3-PhDBF generally increases with rising thermal maturity. Based on the distributions of PhDBFs in the geological samples, the relative abundances of 2-PhDBF, 3-PhDBF and 4-PhDBF are controlled by the thermal maturity of organic matter. The thermodynamic stability of 4-PhDBF is

Table 2
Absolute concentrations of phenyldibenzofurans, methyldibenzofurans, and related parameters of coals.

Sample Name	C_{31} 22S/(22S + 22R) hopane	C_{29} ααα 20S/(20S + 20R) sterane	F_1	F_2	Pr/Ph	PhFR-1	PhFR-2	4-PhDBF/1-PhDBF	4-MDBF/1-MDBF	PhDBFs (μg/g C_{org})	MDBFs (μg/g C_{org})
CB2-1	0.61	0.27	0.23	0.14	7.34	0.59	0.41	0.99	1.70	0.06	3.51
AK1-1	0.60	0.39	0.33	0.21	7.41	1.21	0.67	2.56	1.59	0.67	11.7
BW1-1	0.61	0.28	0.22	0.15	7.91	1.00	0.53	6.92	0.97	0.38	11.3
CB1-1	0.61	0.36	0.21	0.14	7.87	0.65	0.43	2.85	2.16	0.07	10.9
DT4-1	0.60	0.43	0.29	0.17	7.85	0.97	0.48	0.86	1.91	0.80	14.4
BW1-2	0.59	0.37	0.24	0.16	8.82	0.65	0.47	5.05	1.28	0.54	28.3
CB1-2	0.60	0.43	0.21	0.13	7.80	0.89	0.53	1.67	2.15	0.47	12.4
AS1-1	0.51	0.47	0.52	0.35	4.95	1.83	1.25	17.3	1.16	1.47	26.8
CB2-2	0.59	0.45	0.28	0.19	7.80	0.47	0.38	5.20	1.62	0.63	27.7
AK5-1	0.57	0.49	0.47	0.30	5.69	2.18	1.54	14.9	1.70	0.35	31.8
DT5-1	0.60	0.45	0.21	0.14	8.46	0.73	0.54	3.18	0.77	0.14	2.35
AK1-2	0.59	0.44	0.24	0.17	7.91	0.57	0.41	6.32	1.29	1.44	32.3
CB1-3	0.59	0.44	0.36	0.26	6.76	0.64	0.47	2.93	1.26	1.67	22.3
AK1-3	0.58	0.46	0.43	0.33	6.53	1.44	0.96	11.5	2.14	0.06	1.41
BDS24	0.58	0.42	0.45	0.25	0.77	0.99	0.61	9.18	1.35	0.14	0.33
BDS14	0.59	0.41	0.48	0.26	0.99	0.93	0.58	8.43	1.92	0.16	0.82
LXS11	0.62	0.41	0.50	0.28	1.41	0.99	0.60	9.91	0.96	0.56	3.22
LXS15	0.59	0.40	0.54	0.31	1.47	0.87	0.53	13.9	1.76	0.31	4.02
LXS8	0.58	0.48	0.55	0.31	0.96	0.96	0.59	13.3	1.54	0.25	2.79
XXS10	0.60	0.44	0.50	0.27	2.00	1.01	0.65	12.1	1.71	0.67	4.47
XXS2	0.59	0.41	0.77	0.44	1.39	12.3	6.10	28.3	0.52	0.07	0.63
LLS25	0.56	0.46	0.78	0.44	1.20	14.2	6.62	29.9	0.27	0.14	0.40
LLS26	0.56	0.43	0.76	0.43	1.33	9.48	5.17	25.8	0.42	0.67	0.05
LLS5	0.56	0.43	0.77	0.44	1.14	10.8	6.12	15.2	0.39	0.01	0.15
HCS1	0.61	0.43	0.87	0.53	0.77	22.3	9.46	26.4	0.42	0.00	0.22
HCS13	0.59	0.47	0.86	0.51	0.49	16.8	8.52	29.3	0.60	0.32	2.31
HCS4	0.53	0.40	0.87	0.52	0.70	32.1	13.9	23.4	0.40	0.01	0.06
PXS22	0.59	0.47	0.47	0.26	1.40	1.06	0.66	9.29	1.62	0.21	2.08
PXS6	0.59	0.45	0.48	0.26	1.10	1.14	0.69	9.77	2.04	0.34	3.46
YPS9	0.53	0.46	0.78	0.43	0.73	8.16	4.57	18.5	0.58	0.01	0.37

F_1: (3-MP + 2-MP)/(1-MP + 2-MP + 3-MP + 9-MP); F_2: 2-MP/(1-MP + 2-MP + 3-MP + 9-MP); Pr/Ph: pristane/phytane; PhFR-1: 4-phenyldibenzofuran/2-phenyldibenzofuran; PhFR-2: 4-phenyldibenzofuran/(2-phenyldibenzofuran + 3-phenyldibenzofuran); PhDBF: phenyldibenzofuran; 4-MDBF/1-MDBF: 4-methyldibenzofuran/1-methyldibenzofuran; PhDBFs: the sum of the absolute concentrations of 1-, 2-, 3- and 4-phenyldibenzofurans; MDBFs: the sum of the absolute concentrations of 1-, 2-, 3- and 4-methyldibenzofurans.

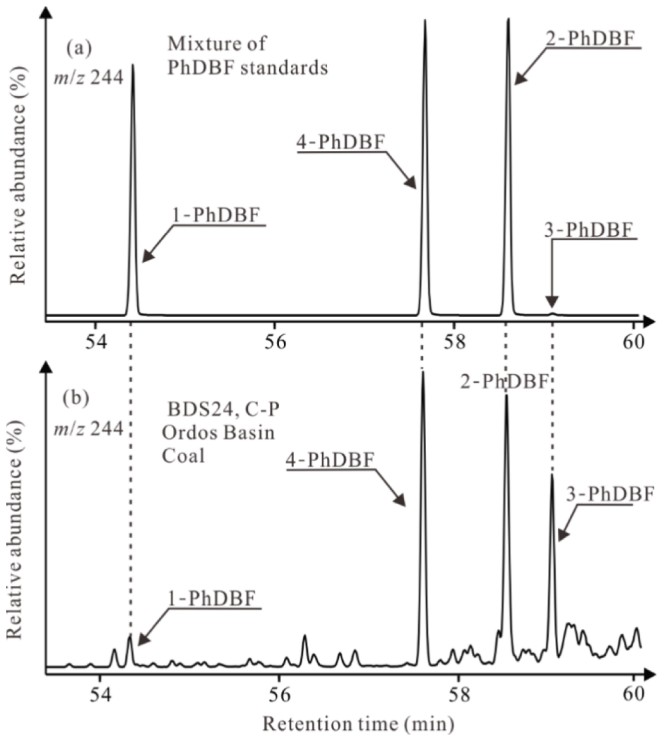

Fig. 2. Identification of the phenyldibenzofuran isomers in the coal.

Table 3
Thermodynamic properties of phenyldibenzofurans isomers. ΔE, ΔU, ΔH and ΔG are expressed relative to the most stable isomer.

Isomer	ΔE (kcal/mol)	ΔU (kcal/mol)	ΔH (kcal/mol)	ΔG (kcal/mol)
4-PhDBF	0.00	0.00	0.00	0.00
2-PhDBF	0.30	0.30	0.30	0.29
3-PhDBF	0.70	0.72	0.72	0.66
1-PhDBF	1.36	1.36	1.36	1.41

estimated to be higher than that of 2-PhDBF and 3-PhDBF, which is consistent with the calculated thermodynamic result.

In this study, based on geochemical data and theoretical calculations, the previously proposed PhDBF ratios (PhFR-1 = 4-PhDBF/2-PhDBF and

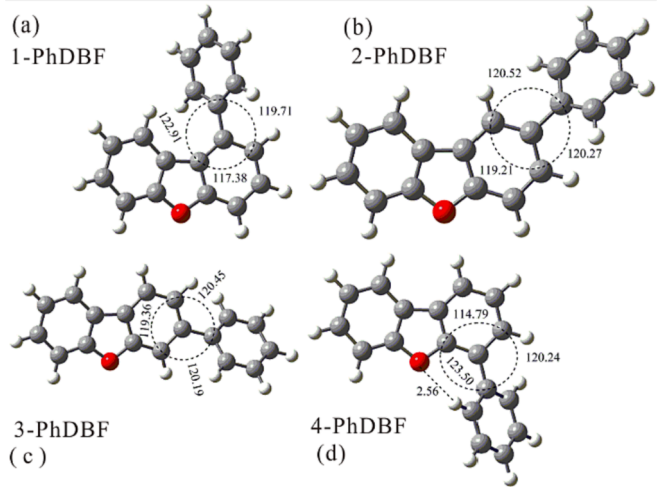

Fig. 3. The geometric optimizations of: (a) 1-PhDBF, (b) 2-PhDBF, (c) 3-PhDBF and (d) 4-PhDBF.

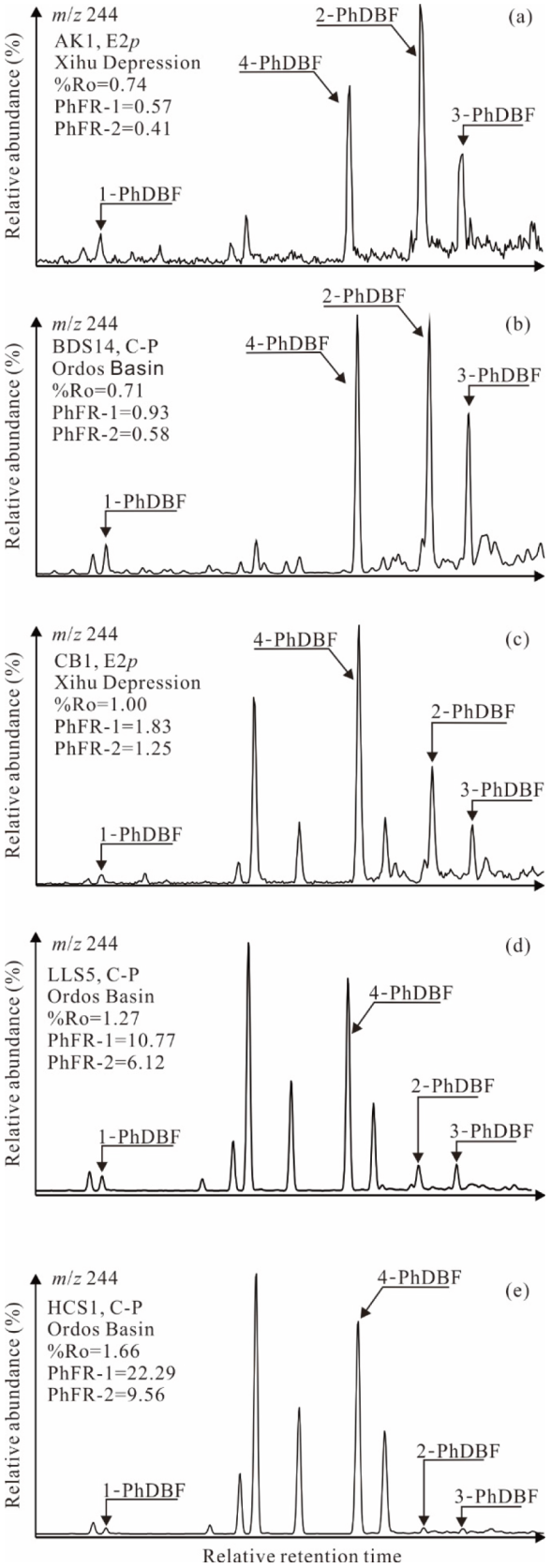

Fig. 4. Distributions of phenyldibenzofurans in the coals with different thermal maturities.

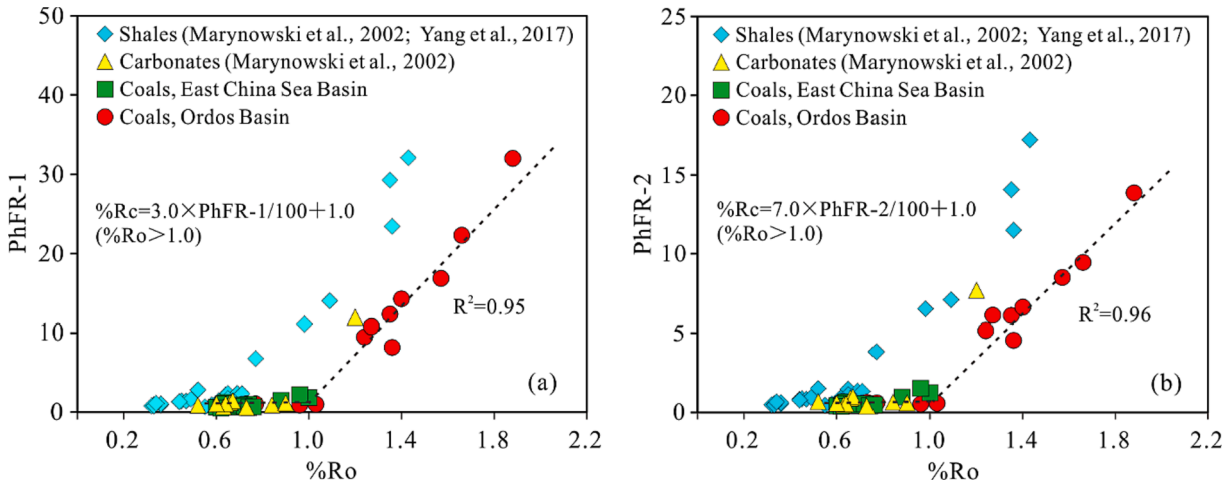

Fig. 5. Correlations of: (a) PhFR-1, (b) PhFR-2 and vitrinite reflectance (%Ro) showing relationship trends of PhDBF ratios with increasing thermal maturity.

PhFR-2 = 4-PhDBF/(2-PhDBF + 3-PhDBF)) are potential maturity indicators. Fig. 5 shows that PhFR-1 and PhFR-2 values of shales, carbonates (Marynowski et al., 2002; Yang et al., 2017) and coals exhibit overall increases with rising thermal maturity, which can be divided into two parts. For the coals and carbonates with maturities < 1.0 %Ro, PhFR-1 and PhFR-2 both remain at low values, which are nearly constant. Interestingly, PhFR-1 and PhFR-2 values obviously increase with rising thermal maturity at high thermal maturity (> 1.0 %Ro). However, for the shales, PhFR-1 and PhFR-2 values are nearly constant < 0.70 % Ro and then gradually increase with increasing thermal maturity. This difference between coals, carbonates and shales may be attributed to the lithology. Previous studies proposed the distribution characteristics of polycyclic aromatic compounds are thermodynamically controlled at high thermal maturity and kinetically controlled at low thermal maturity (Rospondek et al., 2009; Zhu et al., 2019, 2022). The increase in PhFR-1 and PhFR-2 values suggests an increase in the content of the more stable isomer (4-PhDBF) and a decrease in the content of less stable isomers (2-PhDBF and 3-PhDBF). This can be attributed to the formation mechanism of PhDBFs. The less stable isomer (2-PhDBF and 3-PhDBF) due to the lower initial formation enthalpy is able to be formed at low maturity (Yang et al., 2017; Zhu et al., 2019, 2022). With increasing thermal maturity, the less stable isomers (2-PhDBF and 3-PhDBF) may be degraded or probably transform into the more stable isomer (4-PhDBF). Thus, the abundance of 4-PhDBF relative to 2-PhDBF and 3-PhDBF displays an overall increase with increasing thermal maturity.

Fig. 5 shows that PhFR-1 and PhFR-2 of the coals in this study have good linear relationships with the measured vitrinite reflectance (≥ 1.0 %Ro). We preliminarily established the calibrations of PhFR-1 and PhFR-2 against %Ro and the specific relationships are: %Rc = 3.0 × PhFR-1/100 + 1.0 (≥ 1.0 %Ro) and %Rc = 7.0 × PhFR-2/100 + 1.0 (≥ 1.0 %Ro) with correlation coefficients (R^2) up to 0.95 and 0.96, respectively. This indicates PhFR-1 and PhFR-2 are good maturity indicators at high levels of thermal stress.

4.3. Relationships between PhDBF ratios and selected molecular maturity indicators

The C_{31} 22S/(22S + 22R) hopane ratio is a commonly used thermal maturity parameter for immature to the early oil generation stages, which reaches equilibrium at 0.57–0.62 (Seifert and Moldowan, 1980; Peters et al., 2005). The C_{29} ααα 20S/(20S + 20R) sterane ratio is an effective maturity indicator, whilst a ratio in the range of 0.52–0.55 suggests that the main phase of oil generation has been reached or surpassed (Seifert and Moldowan, 1986). As can be seen from Fig. 6a,b, PhFR-1 and PhFR-2 values both show increases when C_{31} 22S/(22S + 22R) hopane ratio reaches the equilibrium values (0.57–0.62). The PhFR-1 and PhFR-2 values of the coals retain low constant values when the C_{29} ααα 20S/(20S + 20R) sterane ratio = 0.27–0.39. PhFR-1 and PhFR-2 values also show increases with C_{29} ααα 20S/(20S + 20R) sterane ratio = 0.40–0.49 (Fig. 6c,d). Significantly, for the coal samples with high maturity (> 1.0 %Ro), C_{29} ααα 20S/(20S + 20R) sterane ratios (0.40–0.49) are lower than the equilibrium values (0.52–0.55). The reason may be that high thermal maturity results in a decrease of C_{29} ααα 20S/(20S + 20R) sterane ratio (Peters et al., 1990). These results are consistent with the trend of PhFR-1 and PhFR-2 values with increasing vitrinite reflectance, which suggests that PhFR-1 and PhFR-2 are particularly useful maturity indicators at higher levels of thermal stress where C_{31} 22S/(22S + 22R) hopane and C_{29} ααα 20S/(20S + 20R) sterane ratios are not available.

Kvalheim et al. (1987) proposed the methylphenanthrene (MP) distribution fractions (F_1 and F_2) as effective maturity indicators for coals, which can be expressed as F_1 = (3-MP + 2-MP)/(1-MP + 2-MP + 3-MP + 9-MP) and F_2 = 2-MP/(1-MP + 2-MP + 3-MP + 9-MP). Fig. 6e–h show that PhFR-1 and PhFR-2 values of the coals both display overall increases with increasing F_1 and F_2 values, which contain two parts. The PhFR-1 and PhFR-2 values of the coals remain at a low constant value at F_1 = 0.21–0.55 and F_2 = 0.13–0.35 (< 1.0 %Ro). Notably, PhFR-1 and PhFR-2 values then gradually increase with increasing F_1 and F_2 values (F_1 > 0.55 and F_2 > 0.35) after 1.0 %Ro. The observed phenomena are identical to the trend of PhFR-1 and PhFR-2 values with increasing vitrinite reflectance. Thus, PhFR-1 and PhFR-2 are correlated with the widely used thermal maturity parameters, suggesting that they are indicators for quantitatively assessing thermal maturity.

4.4. Comparison of phenyldibenzofurans and methyldibenzofurans

In order to investigate the generative mechanism of PhDBFs in the geosphere, the distribution patterns of PhDBFs and MDBFs were compared. Fig. 7 illustrates the comparison of the 4-PhDBF/1-PhDBF and 4-MDBF/1-MDBF ratios to the vitrinite reflectance. The 4-MDBF/1-MDBF ratios of mudstones, shales and coals from Radke et al. (2000) and the present study exhibit overall decreases with increasing thermal maturity, which can be divided into two parts (Fig. 7a). There is no evident regular trend for 4-MDBF/1-MDBF with increasing thermal maturity at 0.60–0.80 %Ro. Significantly, 4-MDBF/1-MDBF ratios gradually decrease with the increase of vitrinite reflectance > 0.80 %Ro, which is inconsistent with phenomenon observed by Li et al. (2011, 2018). 4-MDBF is thermodynamically more stable than 1-MDBF (Radke et al., 2000; Li et al., 2011), causing the increase of 4-MDBF/1-MDBF with increasing thermal maturity, which contradicts the result of this

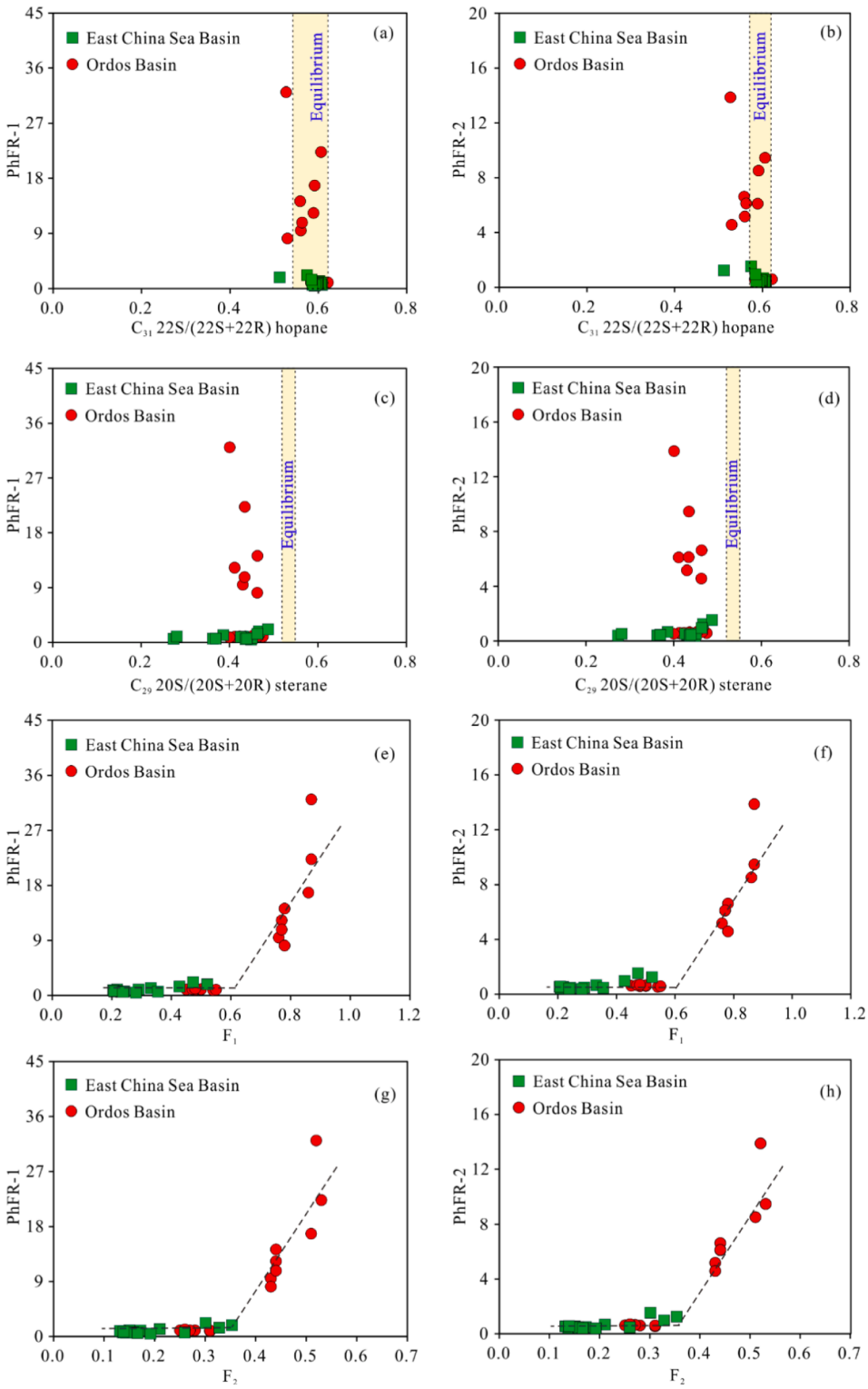

Fig. 6. Correlations of C_{31} 22S/(22S + 22R) hopane, C_{29} ααα 20S/(20S + 20R) sterane, F_1, F_2 and PhDBF ratios of the coals showing the relationships between PhDBF ratios and the other widely used thermal maturity indicators.

study. These observations illustrate that the main controlling factor for the distributions of 4-MDBF and 1-MDBF may not be thermal maturity. However, contrary to the behavior of 4-MDBF/1-MDBF, the 4-PhDBF/1-PhDBF values of carbonates and shales from Marynowski et al. (2002) and coals from this study exhibit general increases with the rising vitrinite reflectance values (Fig. 7b). This phenomenon suggests that the relative abundances of 1-PhDBF and 4-PhDBF are controlled by the thermal maturity and 4-PhDBF is more stable than 1-PhDBF, which is consistent with the calculated thermodynamic data. However, 4-PhDBF/1-PhDBF is difficult to use as a maturity parameter due to the low abundance of 1-PhDBF. These results suggest that PhDBFs do not behave to the same as MDBFs with increase in thermal maturity. This is most likely attributed to their different formation mechanisms.

The absolute concentrations of PhDBFs and MDBFs with Pr/Ph were

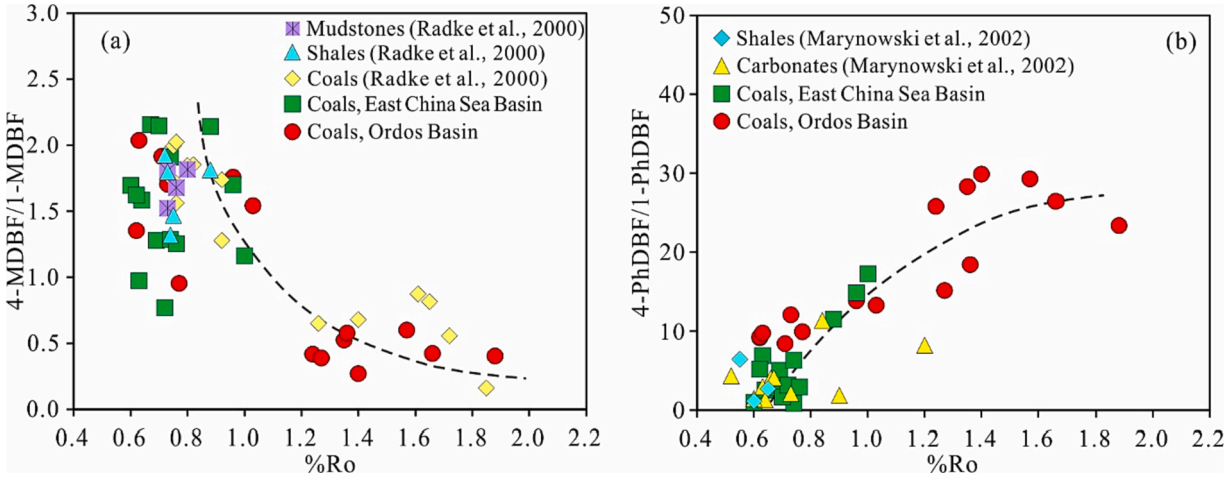

Fig. 7. Correlations of: (a) 4-MDBF/1-MDBF, (b) 4-PhDBF/1-PhDBF and vitrinite reflectance showing the comparison of phenyldibenzofurans and methyldibenzofurans with increasing thermal maturity.

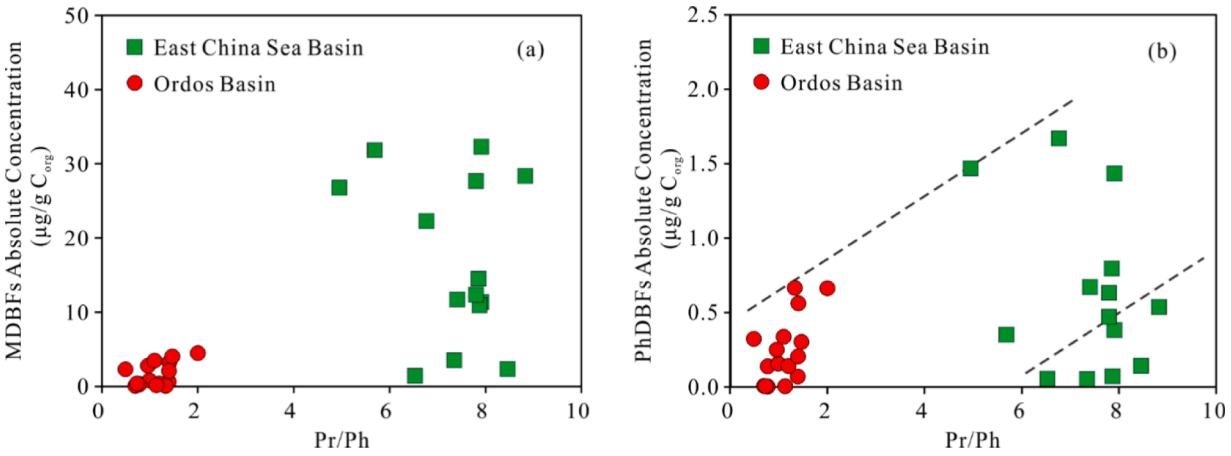

Fig. 8. Correlations of: (a) the absolute concentration of MDBFs, (b) the absolute concentration of PhDBFs and Pr/Ph of the coals showing their formations in different depositional environments.

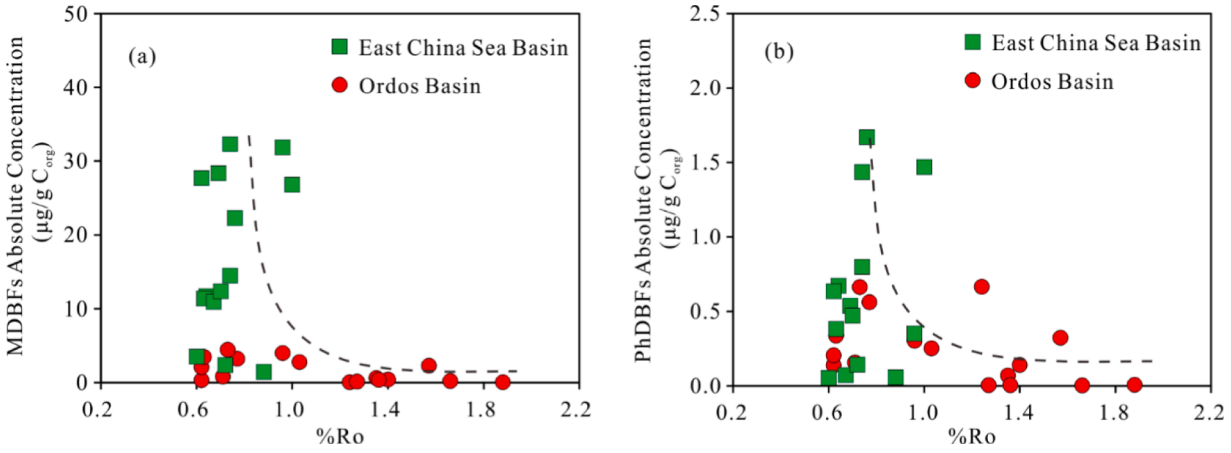

Fig. 9. Correlations of: (a) the absolute concentration of MDBFs, (b) the absolute concentration of PhDBFs and vitrinite reflectance of the coals showing relationship trends of MDBFs and PhDBFs concentrations with increasing thermal maturity.

combined in order to study their depositional environments of their formations due to Pr/Ph been widely representative of the paleo-redox property of ancient environments (Didyk et al., 1978; Hughes et al., 1995). Fig. 8a illustrated that the coals from the Xihu Depression with high Pr/Ph ratios (4.95–8.82) have high absolute concentrations of MDBFs (1.41–32.3 μg/g C_{org}). In contrast, the coal samples collected from the Ordos Basin, the absolute MDBFs concentrations are very low (0.05–4.08 μg/g C_{org}), which are characterized by lower Pr/Ph values (<

2.0). This suggests oxic conditions may contribute to the generation of MDBFs, which is consistent with previous studies (Fan et al., 1991; Radke et al., 2000; Li and Ellis, 2015). Interestingly, the observed behavior of PhDBFs is similar to that of MDBFs. The absolute concentrations of PhDBFs display a general increase with increasing Pr/Ph value (Fig. 8b). This indicates that an oxic sedimentary environment is likely more beneficial to the generation of PhDBFs. Although we did not make the formation mechanism of PhDBFs clear in this paper, the similarities of MDBFs and PhDBFs under different formation environments and their different behaviors with increasing thermal maturity are presented.

4.5. Origin of phenyldibenzofurans

The formation mechanism and origins of PhDBFs are still controversial. Marynowski et al. (2002) suggested that PhDBFs might be formed during diagenetic/catagenetic oxidation since sedimentary rocks affected by hydrothermal fluids have significant concentrations of PhDBFs. However, Grafka et al. (2015) found that the shales affected by hydrothermal oxidation contain very low concentrations of PhDBFs. Interestingly, the absolute concentrations of PhDBFs in the coals from the Xihu Depression are high, which were not altered by hydrothermal fluids. However, PhDBFs occur in the coals from the Ordos Basin with relatively low concentrations, which were affected by hydrothermal oxidation. The results show that the generative mechanism of PhDBFs is not mainly controlled by hydrothermal fluid alteration. Notably, most rock samples in the study of Marynowski et al. (2002) are characterized by low maturities (< 0.70 %Ro), while the samples reported by Grafka et al. (2015) are highly mature with vitrinite reflectances > 1.13 %Ro. This demonstrates that thermal maturity may be the main controlling factor in the formation of PhDBFs.

The absolute concentrations of MDBFs and PhDBFs were compared with increasing vitrinite reflectance in order to discuss the origin of PhDBFs. The MDBFs concentrations in less mature coals (< 0.70 %Ro) are very high, while MDBFs concentrations rapidly decrease with increasing vitrinite reflectance (> 0.90 %Ro) (Fig. 9a). Interestingly, the behavior of PhDBFs is similar to MDBFs. The coals with maturities < 0.70 %Ro contain high abundances of PhDBFs, and then follow a general decrease with increasing thermal maturity (> 0.9 %Ro) (Fig. 9b). The results indicate that MDBFs in coals are likely formed during the diagenesetic or early catagenesis stages and degrade or transform into other compounds during the high maturity stage.

Marynowski et al. (2002) proposed that PhDBFs may be intermediates in the process of transformation of dibenzofuran (DBF) into more complex heterocyclic aromatic compounds, for example triphenyleno[1,12-*bcd*]furan and benzobisbenzofuran. Coincidentally, we detected triphenyleno[1,12-*bcd*]furan and benzobisbenzofuran with high abundances in the coals with high thermal maturity (> 1.0 %Ro). However, these compounds are absent in the coals with low thermal maturity (< 0.70 %Ro). These observations demonstrated that PhDBFs may be formed during diagenetic and early catagenetic period, and are intermediates in the generating processes of more condensed aromatic compounds at high thermal maturity, e.g., triphenyleno[1,12-*bcd*]furan and benzobisbenzofurans. More work should be conducted to have a deeper insight into the geochemical fate of PhDBFs.

5. Conclusions

All four PhDBF isomers have been unequivocally identified in coals for the first time by injection of commercially available standards. PhDBF isomers occur in all coals from the Xihu Depression and the Ordos Basin. For high maturity coals (> 1.0 %Ro), the abundances of 2-PhDBF and 3-PhDBF relative to 4-PhDBF show general increases with increasing thermal maturity. Judging from the thermodynamic stabilities and distributions of PhDBFs in the coals, the previously proposed PhDBF ratios (PhFR-1 and PhFR-2) are useful maturity indicators at higher levels of thermal stress. Two preliminary calibrations of PhDBF ratios against the measured %Ro were established as follows: %Rc = 3.0 × PhFR-1/100 + 1.0 (≥ 1.0 %Ro) and %Rc = 7.0 × PhFR-2/100 + 1.0 (≥ 1.0 %Ro) and their correlation coefficients are up to 0.95 and 0.96, respectively. PhFR-1 and PhFR-2 have good correlations with previously widely used thermal maturity indicators, for example C_{31} 22S/(22S + 22R) hopane, C_{29} ααα 20S/(20S + 20R) sterane, F_1 and F_2. 4-PhDBF/1-PhDBF generally increases with rising thermal maturity, while 4-MDBF/1-MDBF decreases. The oxic depositional conditions may have contributed to the generation of MDBFs and PhDBFs. PhDBFs in coals have a diagenesis/catagenesis origin and may be the intermediates in the formation of triphenyleno[1,12-*bcd*]furan and benzobisbenzofurans. This paper attempts to provide a better understanding of occurrence and origin of PhDBFs in sediments.

Declaration of Competing Interest

The authors declare that they have no known competing financial interests or personal relationships that could have appeared to influence the work reported in this paper.

Data availability

The authors do not have permission to share data.

Acknowledgements

The authors are grateful to SINOPEC Shanghai Offshore Oil & Gas Company for supplying the samples. We are grateful for the help of Lei Zhu and Shengbao Shi with the GC–MS analysis. The authors would like to extend our appreciation to the editors Dr. John Volkman, Professor Kliti Grice, the reviewer Dr. Se Gong and anonymous reviewers for their constructive suggestions and comments which improved the final manuscript.

References

Asif, M., Alexander, R., Fazeelat, T., Grice, K., 2010. Sedimentary processes for the geosynthesis of heterocyclic aromatic hydrocarbons and fluorenes by surface reactions. Organic Geochemistry 41, 522–530.

Born, J.G.P., Mulder, R.L.P., 1989. Formation of dibenzodioxins and dibenzofurans in homogenous gas-phase reactions of phenols. Chemosphere 19, 401–406.

Chen, L., 1998. Depositional environment evolution of Pinghu Formation in Xihu Depression, the East China Sea. Marine Geology and Quaternary Geology 18, 70–79 in Chinese with English abstract.

Cheng, X., Hou, D., Zhao, Z., Chen, X., Diao, H., 2019. Sources of natural gases in the Xihu Sag, East China Sea Basin: Insights from stable carbon isotopes and confined system pyrolysis. Energy & Fuel 33, 2166–2175.

Cheng, X., Hou, D., Zhou, X., Liu, J., Diao, H., Jiang, Y., Yu, Z., 2020. Organic geochemistry and kinetics for natural gas generation from mudstone and coal in the Xihu Sag, East China Sea Shelf Basin, China. Marine and Petroleum Geology 118, 104405.

Dai, J., Li, J., Luo, X., Zhang, W., Hu, G., Ma, C., Guo, J., Ge, S., 2005. Stable carbon isotope compositions and source rock geochemistry of the giant gas accumulations in the Ordos Basin, China. Organic Geochemistry 36, 1617–1635.

Didyk, B.M., Simoneit, B.R.T., Brassell, S.C., Eglinton, G., 1978. Organic geochemical indicators of palaeoenvironmental conditions of sedimentation. Nature 272, 216–222.

Ding, W., Zhu, D., Cai, J., Gong, M., Chen, F., 2013. Analysis of the developmental characteristics and major regulating factors of fractures in marine–continental transitional shale-gas reservoirs: A case study of the Carboniferous-Permian strata in the southeastern Ordos Basin, central China. Marine and Petroleum Geology 45, 121–133.

Fan, P., Philp, R.P., Li, Z., Yu, X., Ying, G., 1991. Biomarker distributions in crude oils and source rocks from different sedimentary environments. Chemical Geology 93, 61–78.

Fenton, S., Grice, K., Twitchett, R.J., Böttcher, M.E., Looy, C.V., Nabbefeld, B., 2007. Changes in biomarker abundances and sulfur isotopes of pyrite across the Permian-Triassic (P/Tr) Schuchert Dal section (East Greenland). Earth and Planetary Science Letters 262, 230–239.

Fields, E.K., Meyerson, S., 1967. Arylation by aromatic nitro compounds at high temperatures. II. nitrobenzene alone and with benzene and benzene-d6. Journal of the American Chemical Society 89, 3224–3228.

Grafka, O., Marynowski, L., Simoneit, B.R.T., 2015. Phenyl derivatives of polycyclic aromatic compounds as indicators of hydrothermal activity in the Silurian black

siliceous shales of the Bardzkie Mountains, Poland. International Journal of Coal Geology 139, 142–151.
Hu, G., Li, J., Shan, X., Han, Z., 2010. The origin of natural gas and the hydrocarbon charging history of the Yulin gas field in the Ordos Basin, China. International Journal of Coal Geology 81, 381–391.
Hughes, W.B., Holba, A.G., Dzou, L.I.P., 1995. The ratios of dibenzothiophene to phenanthrene and pristane to phytane as indicators of depositional environment and lithology of petroleum source rocks. Geochimica et Cosmochimica Acta 59, 3581–3598.
Kilby, W.E., 1988. Recognition of vitrinite with non-uniaxial negative reflectance characteristics. International Journal of Coal Geology 9, 267–285.
Kováts, E., 1958. Gas-chromatographische charakterisierung organischer verbindungen. Teil 1: Retentionsindices aliphatischer halogenide, alkohole, aldehyde und ketone. Helvetica Chimica Acta 41, 1915–1932.
Kruge, M.A., Mukhopadhyay, P.K., Goodarzi, F., Calder, J.H., 2000. Determination of thermal maturity and organic matter type by principal components analysis of the distributions of polycyclic aromatic compounds. International Journal of Coal Geology 43, 27–51.
Kvalheim, O.M., Christy, A.A., Telnaes, N., Bijorseth, A., 1987. Maturity determination of organic matter in coals using the methylphenanthrene distribution. Geochimica et Cosmochimica Acta 51, 1883–1888.
Lee, M.L., Vassilaros, D.L., White, C.M., 1979. Retention indices for programmed-temperature capillary-column gas chromatography of polycyclic aromatic hydrocarbons. Analytical Chemistry 51, 768–773.
Li, D., 1995. Theory and practice of petroleum geology in China. Earth Science Frontiers 2, 15–19 in Chinese with English abstract.
Li, M., Ellis, G.S., 2015. Qualitative and quantitative analysis of dibenzofuran, alkyldibenzofurans, and benzo[*b*]naphthofurans in crude oils and source rock extracts. Energy & Fuel 29, 1421–1430.
Li, S., Li, C., 2003. Analysis on the petroleum resource distribution and exploration potential of the Xihu Depression, the East China Sea. Petroleum Geology and Experiment 25, 721–728 in Chinese with English abstract.
Li, C., Li, S., Xu, H., 2004. Petroleum geologic characteristics and exploration potential of middle–lower Eocene Baoshi Formation in the Xihu Sag. Marine Geology and Quaternary Geology 24, 81–87 in Chinese with English abstract.
Li, M., Wang, T., Yang, F., Shi, Y., 2011. Molecular tracers for filling pathway in condensate pools: Alkyldibenzofuran. Journal of Oil and Gas Technology 33, 6–17 in Chinese with English abstract.
Li, M., Zhong, N., Shi, S., Zhu, L., Tang, Y., 2013. The origin of trimethyldibenzothiophenes and their application as maturity indicators in sediments from the Liaohe Basin, East China. Fuel 103, 299–307.
Li, M., Liu, X., Wang, T., Jiang, W., Fang, R., Yang, L., Tang, Y., 2018. Fractionation of dibenzofurans during subsurface petroleum migration: Based on molecular dynamics simulation and reservoir geochemistry. Organic Geochemistry 115, 220–232.
Liu, X., Li, M., Tang, Y., Zhu, Z., Qi, L., Shi, S., Leng, J., Han, Q., Xiao, H., 2020. Maturity indicators and its mechanism of triphenyls in sedimentary organic matter: Based on geochemical data and quantum chemical calculation. Geochimica 49, 218–226 in Chinese with English abstract.
Marynowski, L., Simoneit, B.R.T., 2009. Widespread Upper Triassic to Lower Jurassic wildfire records from Poland: Evidence from charcoal and pyrolytic polycyclic aromatic hydrocarbons. PALAIOS 24, 785–798.
Marynowski, L., Czechowski, F., Simoneit, B.R.T., 2001. Phenylnaphthalenes and polyphenyls in Palaeozoic source rocks of the Holy Cross Mountains, Poland. Organic Geochemistry 32, 69–85.
Marynowski, L., Rospondek, M.J., Meyer zu Reckendorf, R., Simoneit, B.R.T., 2002. Phenyldibenzofurans and phenyldibenzothiophenes in marine sedimentary rocks and hydrothermal petroleum. Organic Geochemistry 33, 701–714.
Meyer zu Reckendorf, R., 1997. Identification of phenyl-substituted polycyclic aromatic compounds in ring furnace gases using GC-MS and GC-AED. Chromatographia 45, 173–182.
Meyer zu Reckendorf, R., 2000. Phenyl-substituted polycyclic aromatic compounds as intermediate products during pyrolytic reactions involving coal tars, pitches and related materials. Chromatographia 52, 67–76.
Ogbesejana, A.B., Bello, O.M., 2020. Distribution and geochemical significance of dibenzofurans, phenyldibenzofurans and benzo[*b*]naphthofurans in source rock extracts from Niger Delta basin, Nigeria. Acta Geochimica 39, 973–987.
Peters, K.E., Moldowan, J.M., Sundararaman, P., 1990. Effects of hydrous pyrolysis on biomarker thermal maturity parameters: Monterey phosphatic and siliceous members. Organic Geochemistry 15, 249–265.
Peters, K.E., Walters, C.C., Moldowan, J.M., 2005. The Biomarker Guide, Biomarkers and Isotopes in Petroleum Exploration and Earth History. Cambridge University Press, New York.
Radke, M., Vriend, S.P., Ramanampisoa, L.R., 2000. Alkyldibenzofurans in terrestrial rocks: influence of organic facies and maturation. Geochimica et Cosmochimica Acta 64, 275–286.
Rospondek, M.J., Marynowski, L., Chachaj, A., Góra, M., 2009. Novel aryl polycyclic aromatic hydrocarbons: Phenylphenanthrene and phenylanthracene identification, occurrence and distribution in sedimentary rocks. Organic Geochemistry 40, 986–1004.
Seifert, W.K., Moldowan, J.M., 1980. The effect of thermal stress on source-rock quality as measured by hopane stereochemistry. Physics and Chemistry of the Earth 12, 229–237.
Seifert, W.K., Moldowan, J.M., 1986. Use of biological markers in petroleum exploration. Methods in Geochemistry and Geophysics 24, 261–290.
Sephton, M.A., Looy, C.V., Veefkind, R.J., Visscher, H., Brinkhuis, H., de Leeuw, J.W., 1999. Cyclic diaryl ethers in a Late Permian sediment. Organic Geochemistry 30, 267–273.
Shuai, Y., Zhang, S., Mi, J., Gong, S., Yuan, X., Yang, Z., Liu, J., Cai, D., 2013. Charging time of tight gas in the Upper Paleozoic of the Ordos Basin, central China. Organic Geochemistry 64, 38–46.
Southwick, P.L., Munsell, M.W., Bartkus, E.A., 1961. Direct aromatic carboxymethylation with chloroacetylpolyglycolic acids. Orientation in dibenzofuran as evidence of a free radical mechanism. Journal of the American Chemical Society 83, 1358–1368.
Tao, Z., Zou, C., 2005. Accumulation and distribution of natural gases in Xihu Sag, East China Sea Basin. Petroleum Exploration and Development 32, 103–110 in Chinese with English abstract.
Van den Dool, H., Kratz, P.D., 1963. A generalization of the retention index system including linear temperature programmed gas-liquid partition chromatography. Journal of Chromatography 11, 463–471.
Yang, Y., Li, W., Ma, L., 2005. Tectonic and stratigraphic controls of hydrocarbon systems in the Ordos Basin: A multicycle cratonic basin in central China. American Association of Petroleum Geologists Bulletin 89, 255–269.
Yang, L., Li, M., Wang, T., Liu, X., Jiang, W., Fang, R., Lai, H., 2017. Phenyldibenzofurans and methyldibenzofurans in source rocks and crude oils, and their implications for maturity and depositional environment. Energy & Fuel 31, 2513–2523.
Yang, S., Li, M., Liu, X., Han, Q., Wu, J., Zhong, N., 2019. Thermodynamic stability of methyldibenzothiophenes in sedimentary rock extracts: Based on molecular simulation and geochemical data. Organic Geochemistry 129, 24–41.
Ye, J., Qing, H., Bend, S.L., Gu, H., 2007. Petroleum systems in the offshore Xihu Basin on the continental shelf of the East China Sea. American Association of Petroleum Geologists Bulletin 91, 1167–1188.
Zhao, J., Zhang, W., Li, J., Cao, Q., Fan, Y., 2014. Genesis of tight sand gas in the Ordos Basin, China. Organic Geochemistry 74, 76–84.
Zhu, Y., Li, Y., Zhou, J., Gu, S., 2012. Geochemical characteristics of Tertiary coal-bearing source rocks in Xihu depression, East China Sea Basin. Marine and Petroleum Geology 35, 154–165.
Zhu, Z., Li, M., Tang, Y., Qi, L., Leng, J., Liu, X., Xiao, H., 2019. Identification of phenyldibenzothiophenes in coals and the effects of thermal maturity on their distributions based on geochemical data and theoretical calculations. Organic Geochemistry 138, 103910.
Zhu, Z., Li, M., Li, J., Qi, L., Liu, X., Xiao, H., Leng, J., 2022. Identification, distribution and geochemical significance of dinaphthofurans in coals. Organic Geochemistry 166, 104399.
Zou, C., Wei, G., Xu, C., Du, J., Xie, Z., Wang, Z., Hou, L., Yang, C., Li, J., Yang, W., 2013. Continuous hydrocarbon accumulation over a large area as a distinguishing characteristic of unconventional petroleum: The Ordos Basin, North-Central China. Earth-Science Reviews 126, 358–369.